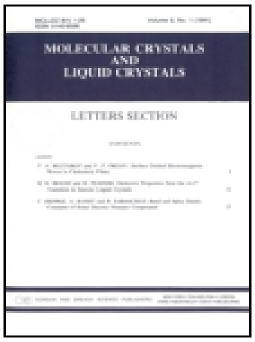

Taylor & Francis
Taylor & Francis Group

Molecular Crystals and Liquid Crystals

ISSN: 1542-1406 (Print) 1563-5287 (Online) Journal homepage: http://www.tandfonline.com/loi/gmcl20

Highly Conductive PEDOT:PSS Film by Post-Treatment with Dimethyl Sulfoxide for ITO-Free Liquid Crystal Display

Tsu-Ruey Chou, Szu-Hua Chen, Yen-Te Chiang, Yi-Ting Lin & Chih-Yu Chao

To cite this article: Tsu-Ruey Chou, Szu-Hua Chen, Yen-Te Chiang, Yi-Ting Lin & Chih-Yu Chao (2015) Highly Conductive PEDOT:PSS Film by Post-Treatment with Dimethyl Sulfoxide for ITO-Free Liquid Crystal Display, Molecular Crystals and Liquid Crystals, 612:1, 201-210, DOI: 10.1080/15421406.2015.1031581

To link to this article: http://dx.doi.org/10.1080/15421406.2015.1031581

Mol. Cryst. Liq. Cryst., Vol. 612: pp. 201–210, 2015
Copyright © Taylor & Francis Group, LLC
ISSN: 1542-1406 print/1563-5287 online
DOI: 10.1080/15421406.2015.1031581

Highly Conductive PEDOT:PSS Film by Post-Treatment with Dimethyl Sulfoxide for ITO-Free Liquid Crystal Display

TSU-RUEY CHOU,[1] SZU-HUA CHEN,[1] YEN-TE CHIANG,[2]
YI-TING LIN,[1] AND CHIH-YU CHAO[1,2,3,*]

[1]Department of Physics, National Taiwan University, Taipei, Taiwan
[2]Institute of Applied Physics, National Taiwan University, Taipei, Taiwan
[3]Molecular Imaging Center, National Taiwan University, Taipei, Taiwan

In this study, a simple method to enhance the conductivity of poly(3,4-ethylenedioxythiphene):poly(styrenesulfonate) (PEDOT:PSS) thin films from 0.7 to 1185 S/cm by post-treatment with dimethyl sulfoxide (DMSO) is demonstrated. After the rubbing technique was applied, the DMSO-treated PEDOT:PSS film was used as both transparent electrode and alignment layer to fabricate ITO-free liquid crystal (LC) cells. The electro-optical properties of LC cells fabricated by rubbed PEDOT:PSS were compared to those constructed by ITO and polyimide. This work indicates that highly conductive PEDOT:PSS film is a promising material for ITO-free LC devices.

Keywords PEDOT:PSS; ITO free; liquid crystal display

Introduction

Optoelectronic devices such as liquid crystal displays (LCDs), organic photovoltaics (OPVs) and organic light-emitting diodes (OLEDs) have received great interest these years due to their mechanical flexibility, light weight, and prospective potential for roll-to-roll manufacturing. Among these devices, LCD has been commercialized at least 30 years and has become the most widely used display in our daily life. Recently, researchers have developed several new modes of liquid crystal (LC) devices to achieve high performance display, e.g., in-plane switching [1], patterned vertical alignment [2], and fringe-field switching [3]. Whatever which modes, LC devices act as a light valve to control the transmission of the backlight. Therefore, transparent electrode is required for the LC device architecture, even in the case of reflective LCDs.

Indium tin oxide (ITO), which could be deposited on both glass and plastic substrate, has been the most commonly used material as transparent electrode for decades. However, the limited indium on earth and the fragile characteristic of ITO thin films increase the cost of LCDs and restrict the applicability of ITO on flexible electronic devices, respectively [4–6]. Furthermore, the total reflection at the glass/ITO interface [7], poor transparency in

---

[*]Address correspondence to Chih-Yu Chao, Department of Physics, National Taiwan University, Taipei 10617, Taiwan. E-mail: cychao@ntu.edu.tw

Color versions of one or more of the figures in the article can be found online at www.tandfonline.com/gmcl.

the blue spectrum [8], and poor adhesion to organic materials degrade the performance of optoelectronic devices using ITO as transparent electrode. These drawbacks make ITO a non-ideal material in the future, and thus searching for an alternative to replace ITO is an unavoidable task.

To date, many materials such as carbon nanotube [9–12], metal nanowires [13, 14], thin metals [15], graphene [16, 17], and conducting polymers [18–20] have been investigated as alternatives to replace ITO. In particular, poly(3,4-ethylenedioxythiophene):poly(styr enesulfonate) (PEDOT:PSS) is one of the most potential material due to its excellent mechanical flexibility, good thermal stability, and high transparency in the visible range. It can be dispersed in water and several organic solvents and hence PEDOT:PSS films could be prepared by simple solution processes such like spin coating or inject printing [21–23]. However, the conductivity of pristine PEDOT:PSS film, typically below 1 S/cm, is extremely lower than that of the commercialized ITO, which makes it inappropriate for practical applications. The insulating PSS, which makes the conductive PEDOT to be dispersed easily in water, is the main reason for the low conductivity of PEDOT:PSS films. In order to improve the conductivity of PEDOT:PSS, several methods have been reported, including doping additional organic compounds with their boiling points higher than the boiling point of water, such as dimethyl sulfoxide (DMSO) [24], ionic liquid [25], dimethyl sulfate [26], or polyol [27], into PEDOT:PSS aqueous solution and processing post treatment of PEDOT:PSS films with cosolvents [28], ethylene (EG) [29], salt [30], or inorganic acid [31]. Generally speaking, doping polar solvents into PEDOT:PSS leads to morphology changes including extended grain size and better interconnection between PEDOT chains; whereas post treatment usually results in both morphology changes and the removal of unwanted PSS on the film surface. Therefore, methods including post treatment usually show better results than those simply using additives to improve the conductivity of PEDOT:PSS films.

In this study, the conductivity enhancement of highly conductive PEDOT:PSS films prepared from the Clevios PH 1000 aqueous solution through the post-treatment with DMSO was performed. The conductivity enhanced greatly by four orders of magnitude, which is attributed to the removal of PSS on the surface and the conformational change of the PEDOT:PSS film. After rubbing with a polyester cloth, the DMSO-treated highly conductive PEDOT:PSS films reveal uniform planer alignment which could be used as both transparent electrode and alignment layer in the LC device. Measured electro-optical properties show similar characteristics compared with those LC cells assembled by the polyimide (PI) coated ITO glass.

Experimental

The PEDOT:PSS aqueous solution (Clevios PH1000) was purchased from Heraeus Clevios GmbH with a solid concentration 1.0 $\sim$ 1.3 wt% and the weight ratio of PEDOT to PSS was 0.4. DMSO (99.9%, anhydrous) was purchased from Sigma-Aldrich with a water content less than 0.005 wt%. All the materials were used without further purification. The chemical structures of these materials are shown in Scheme 1.

Glass substrates (2.5 × 2.5 cm^2) were cleaned with detergent, acetone, isopropyl alcohol and deionised (DI) water successively. After drying in the oven, glass substrates were treated with air plasma for 4 min to enhance the wettability. Single-layer PEDOT:PSS thin film was deposited on a glass substrate via spin coating at 3000 rpm for 60 s and then annealed at 120°C for 15 min. The PEDOT:PSS aqueous solution was filtered through a

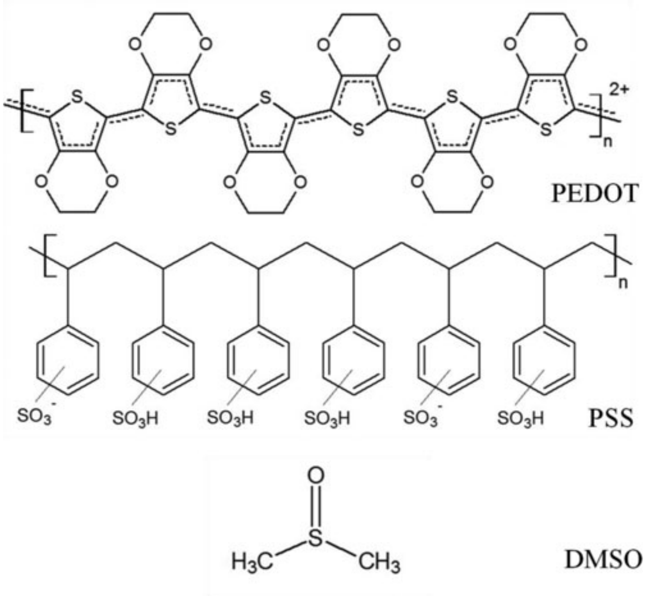

Scheme 1. Chemical structures of PEDOT, PSS and DMSO.

0.45 μm syringe filter prior to spin coating. Next, a small amount of DMSO was dropped directly (hereafter referred as the "drop" method) on the PEDOT:PSS film at 120°C and dried for 15 min. The treated film was then rinsed with DI water several times to remove the excess PSS on the film and finally dried at 120°C for 15 min again. Thicker PEDOT:PSS films were prepared by multiple coatings and treated in the same way described above on each PEDOT:PSS layer.

The sheet resistance (R_s) of PEDOT:PSS films was measured by four point probe method and the electrical conductivity (σ) was calculated by the formula:

$$\sigma = 1\big/(R_s \times d)$$

where d is the film thickness. The surface morphology and thickness of the PEDOT:PSS film were characterized and measured by means of an Park XE-100 atomic force microscope (AFM) operated in tapping mode. Optical transmission spectra were taken using a UV-vis-NIR spectrometer (JASCO V-670).

The empty LC cells were fabricated by two glass substrates coated with highly conductive PEDOT:PSS films. The PEDOT:PSS layer was rubbed with a polyester cloth after post treatment in order to yield a unidirectional planer alignment. Besides, empty LC cells constructed from ITO glass (95 Ω/□) coated with a polyimide layer (AL-12G, Daily-Polymer) were made for comparison. The cell configuration of all samples is 90° twisted nematic (TN) mode with a 4 μm cell gap ensured by silica spacers. Thereafter, nematic LCs (DF-7538A, Daily-Polymer) were injected into empty cells by means of capillary action in isotropic phase. The structure of LC cells fabricated by glass/PEDOT:PSS and glass/ITO/PI are shown in Figure 1.

After sample preparation, polarizing optical microscope (POM) was employed to examine the uniformity of the LC alignment. The voltage-transmittance (V-T) characteristic of each cell from a He-Ne laser source was measured by a silicon photo detector. All cells

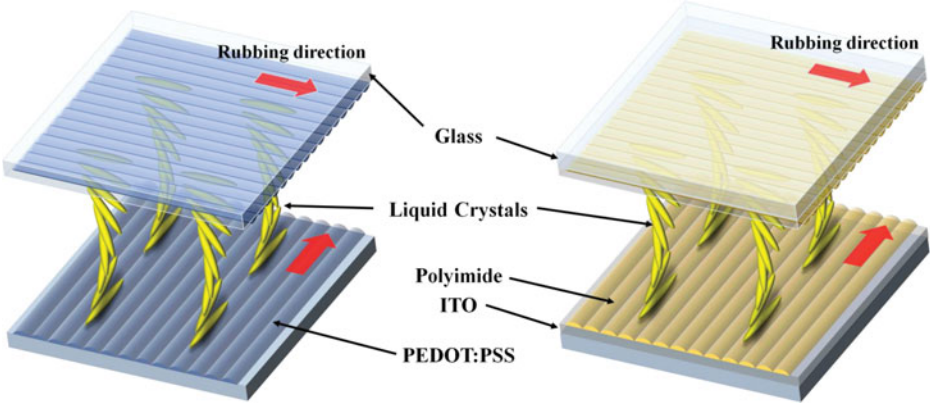

Figure 1. The structure of LC cells fabricated by rubbed highly conductive PEDOT:PSS on glass and polyimide on ITO glass.

were placed between a pair of cross-polarizers and measured by applying a square wave voltage with frequency 1k Hz under the normally white mode.

Results and Discussion

Previous reports have shown that adding a small amount of DMSO or other solvents into high conductive PH 1000 PEDOT:PSS could enhance the conductivity of the PEDOT:PSS film [24]. Besides, some studies showed conductivity enhancement by immersing the dried PEDOT:PSS film into EG or treatment with polar solvent or cosolvents [28, 29, 31]. Therefore, we are interested in which method shows the best result using DMSO. Figure 2 shows the conductivities along with the error bar of pristine PEDOT:PSS and after three conductivity enhance methods using anhydrous DMSO. The "5% DMSO" was done by mixing 5% (v/v) DMSO in the PEDOT:PSS aqueous solution and stirred 24 hr prior to spin coating. The "dip" treatment was performed by immersing the annealed PEDOT:PSS

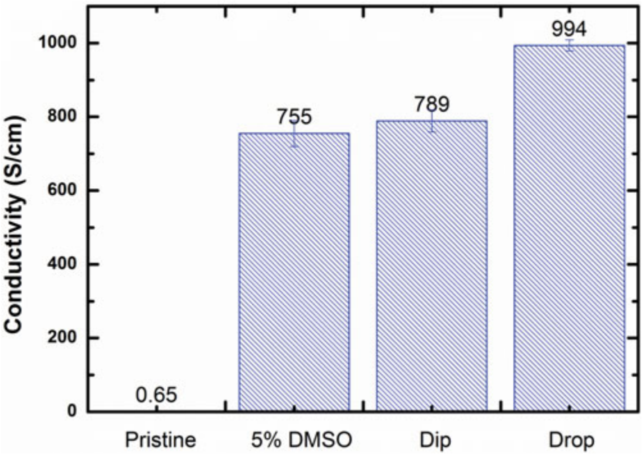

Figure 2. Conductivities of PEDOT:PSS films treated with DMSO by different methods.

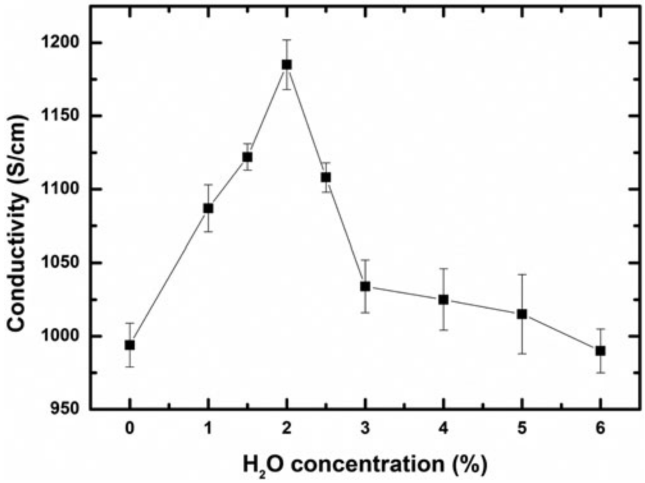

Figure 3. Variation of the conductivity of PEDOT:PSS films treated with DMSO doped with different concentrations of DI water.

film into DMSO at room temperature for 30 min and dried at 120°C for 15 min. The drop method was done by the procedure mentioned in the experimental section. The average conductivity increased from 0.7 S/cm to 755, 789, 994 S/cm for samples added with 5% DMSO, treated with dip method, and treated with drop method, respectively. Obviously, the drop method shows the best result compared with the others.

Previously, Xia and Ouyang reported that the conductivity of PEDOT:PSS film could be enhanced by post-treatment with cosolvents including water, methanol, ethanol, 1,2-dicholobenzene, etc. They carried out a study to find out whether anhydrous methanol or normal methanol (water less than 0.05%) is a better candidate to enhance the conductivity of less conductive PEDOT:PSS (Clevios VP AI4083), which is often used as a buffer layer in OLED or OPV cells. Their results showed that the conductivity of less conductive PEDOT:PSS film treated with normal methanol improved more than those treated with anhydrous methanol [28]. This indicates that even a small amount of water in the normal methanol could influence the result of post-treatment. Motivated by this study, a small amount of DI water was added into the anhydrous DMSO. The concentration of DI water varied from 0 to 6% (v/v). Figure 3 shows the variation of the conductivity of PEDOT:PSS films treated with DMSO doped with different concentration of DI water. The highest conductivity (1185 S/cm) was obtained when the doping concentration was 2%. The conductivity decreased gradually when doping concentration was above 3%.

Various mechanisms have been proposed for the conductivity enhancement of PEDOT:PSS films. For those methods utilizing post-treatment process, two mechanisms contributes to the conductivity enhancement mainly: the removal of those excess PSS on the surface of the film and the conformational change of the PEDOT and PSS chain. The surface of pristine PEDOT:PSS film contains more PSS than the bulk region [32]. Therefore, removing the hygroscopic and insulating PSS on the film surface is crucial to increase the stability and conductivity of the PEDOT:PSS. In this study, the film thickness reduced from 60 nm to 40 nm, which is attributed to the removal of the PSS by DMSO post-treatment. On the other hand, the PEDOT and PSS form a core-shell structure in the pristine film where the core region is conductive PEDOT rich and the shell region is insulating PSS rich

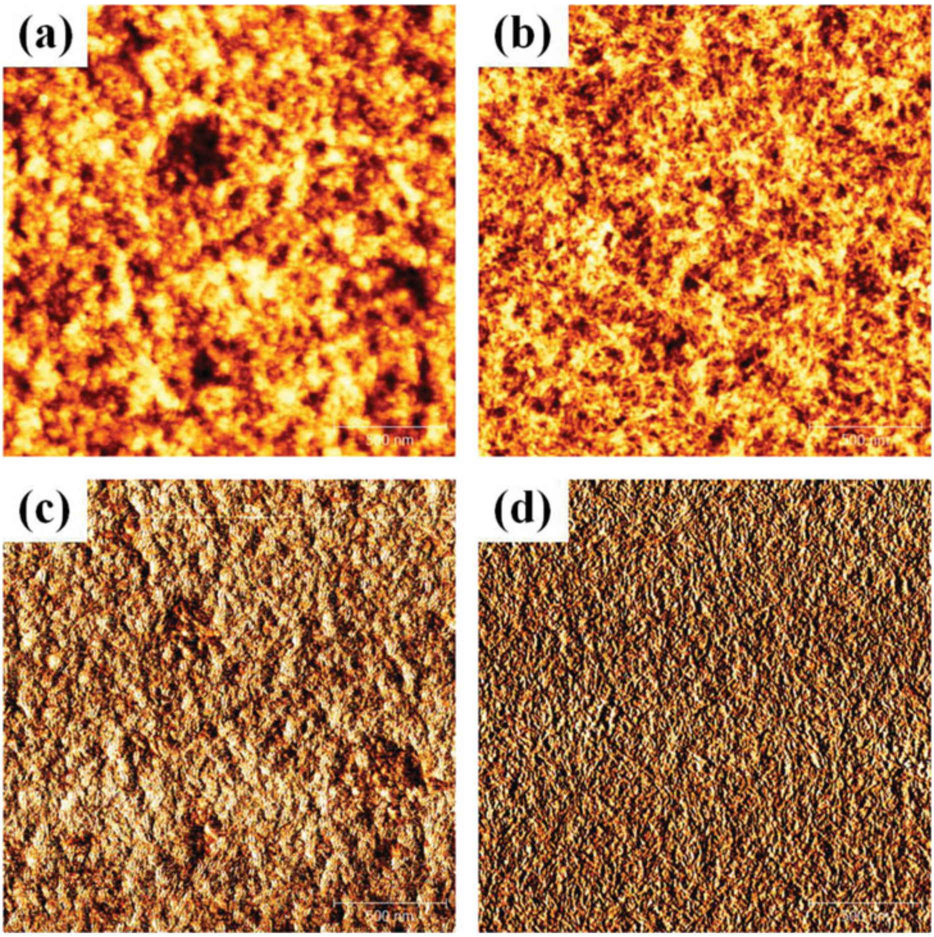

Figure 4. AFM images of PEDOT:PSS films before (a and c) and after (b and d) DMSO drop treatment. (a and b) are surface topography images and (c and d) are phase images. The dimension of these images are 2 μm × 2 μm.

[33]. The conductive core surrounded by the insulating shell makes those carriers on the PEDOT chain hard to transport through the film which results in low conductivity of the pristine film. Surface topography and phase image of the PEDOT:PSS film before and after DMSO drop treatment was captured by AFM, as shown in Figure 4. From Figure 4(a) and 4(b), it is clear that the PEDOT:PSS film turned from a core-shell structure to an entangled wires like structure after the post treatment. This conformational change is attributed to the DMSO post-treatment which reduces the Coulombic attraction between PEDOT and PSS. The reduced attraction results in phase separation between the hydrophobic PEDOT and hydrophilic PSS. Along with the removal of PSS, PEDOT chains turned from coiled to a linear structure, as shown in Figure 4(c) and 4(d). This conformational change reduces the energy barrier of charge hopping on the PEDOT:PSS film which contributes to the conductivity enhancement. The surface roughness (mean roughness) increased from 1.14 nm to 1.56 nm after post treatment, which is still acceptable smoothness.

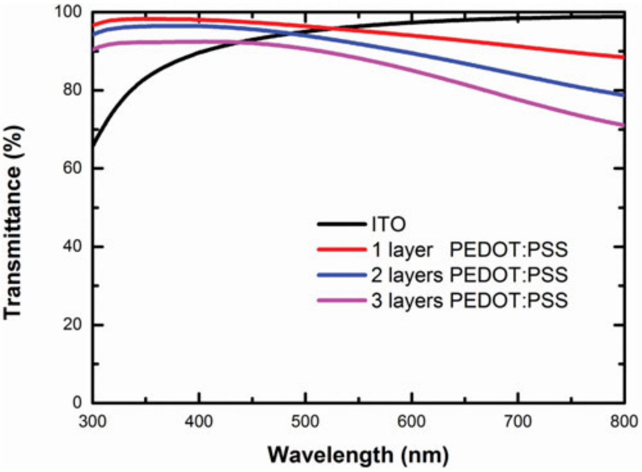

Figure 5. Transmittance spectra of ITO and PEDOT:PSS film with different layers. The sheet resistance of the ITO is 95 Ω/□.

In order to reduce the sheet resistance of the PEDOT:PSS film, multilayer architecture was performed. This can be obtained by spin coating the PEDOT:PSS solution multiple times. The drop treatment was carried out on each layer with 2% DI water doped DMSO. The sheet resistance reduced from 211 to 103 and 67 Ω/□ for single layer, double layers and triple layers, respectively. The conductivity of the third layer is slightly lower, which is similar to the result of other groups [31]. The sheet resistances of multilayer film are comparable or lower than that of ITO substrate usually used for LC device, which has a typical value about 100 Ω/□. Figure 5 presents the transmittance spectra of ITO and DMSO treated PEDOT:PSS films with different layers. The transmittance measured in this study excludes the absorption of the glass substrate due to the glass substrates we used for PEDOT:PSS coating were different from those employed for commercial ITO deposition. The transmittance at 550 nm is 95%, 92% and 88% for single layer, double layers and triple layers, respectively. Thick film results in transmission loss. The sheet resistance and transmittance of the double layer sample are comparable to the ITO (transmittance 96% and $R_s = 95$ Ω/□.) we used for comparison in this study.

In order to align LC molecules on the PEDOT:PSS film, rubbing process was employed. Several materials such as velvet cloth and silicon rubber sheet has been adopted in the rubbing process. In our case, we used a polyester cloth to generate the oriented nanoscale-groove structure on the surface of PEDOT:PSS layer. The surface relief structures of the rubbed PEDOT:PSS films captured by AFM are shown in Figure 6. The orientation of induced grooves is uniformly aligned along the rubbing direction and the depth of the grooves is ranging from a few nanometers to 10 nm. Previous studies have shown that the surface topography of the substrate and the chemical reaction between LC molecules and the alignment layer plays crucial roles in the alignment mechanism [34, 35]. In this study, we speculate that it is the grooved surface of the PEDOT:PSS film and the aromatic rings of PSS which accounts for the liquid crystal alignment.

Figure 7(a) and 7(b) are POM images of LC cells fabricated by highly conductive PEDOT:PSS films with and without the applied external field, respectively. These images were taken under normally black mode. In normally black mode, it would be easy to observe light leakage spots if the TN configuration achieved by rubbed PEDOT:PSS films has some

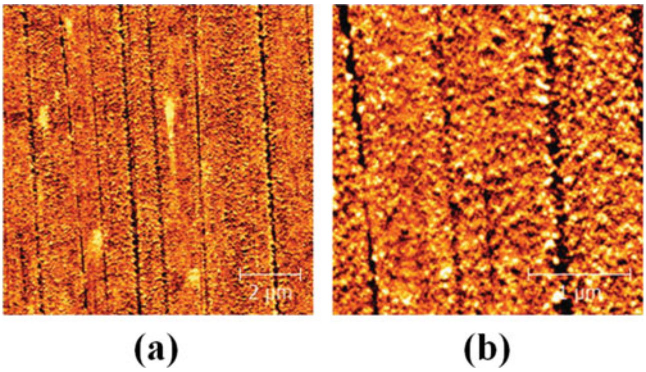

Figure 6. Surface topography of rubbed highly conductive PEDOT:PSS films. The dimension of these images are (a) 10 μm × 10 μm and (b) 3 μm × 3 μm.

defects. In these pictures, uniform dark and bright states were obtained which indicates that the rubbed highly conductive PEDOT:PSS films could align LC molecules well and it would not generate optical observable flaws in the bright state.

In order to investigate the electro-optical properties of the LC cells using rubbed highly conductive PEDOT:PSS as both electrode and alignment layer, V-T curves of these samples were measured. Figure 8 is the normalized transmittance of TN LC cells fabricated by glass/PEDOT:PSS and glass/ITO/PI under applied square wave voltage with the amplitude varying from 0 to 4 V. Measured results indicate that the V-T characteristics of cells constructed by PEDOT:PSS were similar to those of the sample fabricated by the PI coated ITO glass. V-T curve of the sample using PEDOT:PSS was found to shift to higher voltage slightly compared with that using ITO and PI. This is due to the difference in conductivity between PEDOT:PSS and ITO, which leads to a slight voltage drop on the PEDOT:PSS electrode. Threshold voltage and driving voltage are defined as the voltage corresponding to 90% and 10% of the initial transmittance, respectively. The measured threshold and driving voltage were 1.65 V and 2.67 V which were very close to the results of control sample (1.55 V and 2.55 V). Threshold voltage is a key factor in the LCDs industry which corresponds to the power consumption of the LC device. This result shows that LC cells

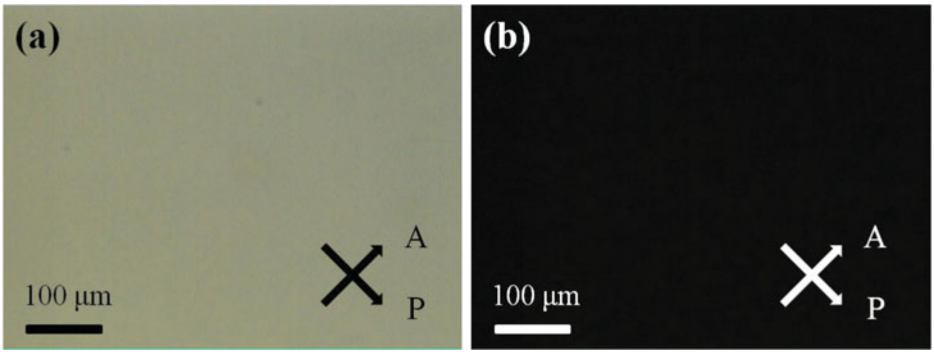

Figure 7. POM images of TN LC cells fabricated by rubbed highly conductive PEDOT:PSS films under normally black mode (a) with and (b) without the applied external field.

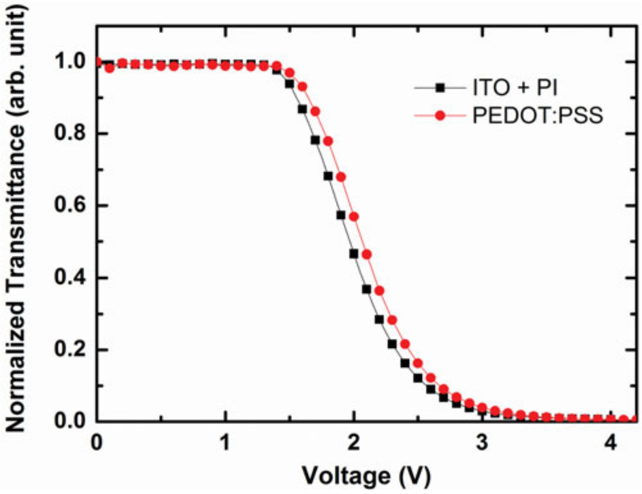

Figure 8. Transmittance of LC cells fabricated by rubbed highly conductive PEDOT:PSS on glass and polyimide on ITO glass under applied square wave voltage.

using PEDOT:PSS films as both transparent electrode and alignment layer possess low power consumption characteristic as a traditional LC device and could further expand the LC device to the flexible electronic field.

Conclusion

In summary, a simple method to enhance the conductivity of PEDOT:PSS thin films by four orders of magnitude is demonstrated. The conductivity of the pristine film increased drastically from 0.7 to 1185 S/cm after film treatment with 2% of DI water doped DMSO. The removal of the insulating PSS together with the re-ordering and conformation changes of the PEDOT and PSS chains are the prime reasons for the conductivity enhancement observed in this study. Uniform LC alignment on the highly conductive PEDOT:PSS film was achieved by using the rubbing technique. Electro-optical properties of TN LC cells fabricated by the rubbed highly conductive PEDOT:PSS film show similar results compared with those fabricated by ITO and polyimide. This work shows the potential and facility of highly conductive PEDOT:PSS films to be used as both transparent electrode and alignment layer in the LC device for ITO-free and flexible LC displays.

Funding

One of the authors (CYC) would like to thank National Taiwan University, National Science Council, and Ministry of Education of the Republic of China for financial supports on this work.

References

[1] Oh-e M., & Kondo K. (1995). *Appl. Phys. Lett., 67*, 3895.
[2] Lee Y. J., Kim Y. K., Jo S. I., Gwag J. S., Yu C. J., & Kim J. H. (2009). *Opt. Express, 17*, 10298
[3] Lee S. H., Lee S. L., & Kim. H. Y. (1998). *Appl. Phys. Lett. 73*, 2881.

[4] Cairns D. R., Witte R. P., Sparacin D. K., Sachsman S. M., Paine D. C., Crawford G. P., & Newton R. R. (2000). *Appl. Phys. Lett. 76*, 1425.

[5] Tao C. S., Jiang J., & Tao M. (2011). *Sol. Energy Mater. Sol. Cells 95*, 3176.

[6] Chipman A. (2007). *Nature 449*, 131.

[7] Saxena K., Jain V. K., & Mehta D. S. (2009). *Opt. Mater 32*, 221.

[8] Phillips J. M., Cava R. J., Thomas G. A., Carter S. A., Kwo J., Siegrist T., Krajewski J. J., Marshall J. H., Peck W. F., & Rapkine D. H. (1995). *Appl. Phys. Lett. 67*, 2246.

[9] Wu Z. C., Chen Z. H., Du X., Logan J. M., Sippel J., Nikolou M., Kamaras K., Reynold J. R., Tanner D. B., Hebard A. F., & Rinzler A. G. (2004). *Science 305*, 1273.

[10] Zhang M., Fang S. L., Zakhidov A. A., Lee S. B., Aliev A. E., Williams C. D., Atkinson K. R., & Baughman R. H. (2005). *Science 309*, 1215.

[11] Gruner G. (2006). *J. Mater. Chem. 16*, 3533.

[12] Joshi P., Zhang L. F., Chen Q. L., Galipeau D., Fong H., & Qiao Q. Q. (2010). *ACS Appl. Mater. Inter. 2*, 3572.

[13] Lee J. Y., Connor S. T., Cui Y., & Peumans P. (2008). *Nano. Lett. 8*, 689.

[14] Hsu P. C., Wang S., Wu H., Narasimhan V. K., Kong D. S., Lee H. R., & Cui Y. (2013). *Nat. Commun.* 3522.

[15] Meiss J., Riede M. K., & Leo K. (2009). *Appl. Phys. Lett. 94*, 013303.

[16] Tung V. C., Chen L. M., Allen M. J., Wassei J. K., Nelson K., Kaner R. B., & Yang Y. (2009). *Nano. Lett. 9*, 1949.

[17] Mei X. G., & Ouyang J. Y. (2011). *Carbon 49*, 5389.

[18] Xia Y. J., Sun K., & Ouyang J. Y. (2012). *Energ. Environ. Sci. 5*, 5325.

[19] Yoo J. E., Lee K. S., Garcia A., Tarver J., Gomez E. D., Baldwin K., Sun Y. M., Meng H., Nguyen Nguyen., & Loo Y. L. (2010). *P. Natl. Acad. Sci. USA 107*, 5712.

[20] Na S. I., Kim S. S., Jo J., & Kim D. Y. (2008). *Adv. Mate. 20*, 4061.

[21] Groenendaal B. L., Jonas F., Freitag D., Pielartzik H., & Reynolds J. R. (2000). *Adv. Mater. 12*, 481.

[22] Cao Y., Yu G., Zhang C., Menon R., & Heeger A. J. (1997). *Synthetic Metals 87*, 171.

[23] Kirchmeyer S., & Reuter K. (2005). *J. Mater. Chem. 15*, 2077.

[24] Laskarakis A., Karagiannidis P. G., Georgiou D., Nikolaidou D. M., & Logothetidis S. (2013). *Thin Solid Films 541*, 102.

[25] Badre C., Marquant L., Alsayed A. M., & Hough L. A. (2012). *Adv. Funct. Mater. 22*, 2723.

[26] Reyes-Reyes M., Cruz-Cruz I., & Lopez-Sandoval R. (2010). *J. Phys. Chem. C 114*, 20220.

[27] Huang J., Miller P. F., Wilson J. S., Mello A. J. de, & Bradley D. D. C. (2005). *Adv. Funct. Mater. 15*, 290.

[28] Sun K., Xia Y. J., & Ouyang J. Y. (2012). *Sol. Energy Mater. Sol. Cells 97*, 89.

[29] Kim Y. H., Sachse C., Machala M. L., May C., Muller-Meskamp L., & Leo K. (2011). *Adv. Funct. Mater. 21*, 1076.

[30] Xia Y. J., & Ouyang J. Y. (2010). *Org. Electron. 11*, 1129.

[31] Xia Y. J., Sun K., & Ouyang J. Y. (2012). *Adv. Mater. 24*, 2436.

[32] Na S. I., Wang G., Kim S. S., Kim T. W, Oh S. H., Yu B. K., Lee T., & Kim D. Y. (2009). *J. Mater. Chem. 19*, 9045.

[33] Lang U., Muller E., Naujoks N., & Dual J. (2009). *Adv. Funct. Mater. 19*, 1215.

[34] Gwag J. S., Yi J., Kwon J. H., Yoneya M., & Yokoyama H. (2011). *J. Appl. Polym. Sci. 119*, 325.

[35] Hoogboom J., Rasing T., Rowan A. E., & Nolte R. J. M. (2006). *J. Mater. Chem. 16*, 1305.